

THE MAGNETIC FIELDS OF ELECTRIC MOTORS AND THEIR EMC

D. Kováč¹⁾, I. Kováčová²⁾

¹⁾ Department of Theoretical Electrical Engineering and Electrical Measurement, FEI TU of Košice, Park Komenského 3, 042 00 Košice, tel.: +421 55 602 2801, E-mail: dobroslav.kovac@tuke.sk

²⁾ Department of Electrical Engineering, Mechatronics and Industrial Engineering, FEI TU of Košice, Letná 2, 042 00 Košice, tel.: +421 55 602 2270, E-mail: irena.kovacova@tuke.sk

Summary This paper deals with the computer analysis of the electromagnetic compatibility (EMC) problems focused on the area of electrical machines, which can also disclose the concerning startling facts. A problem of interference between electric motor and surrounding space caused by the electromagnetic field radiation is discussed too.

1. INTRODUCTION

The possibility of equipment disturbances and errors becomes more serious as a consequence of the electronic circuit complexity growth. According to the new technical legislation and also due to economic consequences, the EMC concept of all products must be strictly observed. It has to start with the equipment performance specifications and finish with the equipment installation procedures.

2. ELECTRIC MOTORS

In most cases a resistor, solenoid or motor, represents the load of the power electrical engineering systems. The most frequent manner of the utilization of electric energy in industry is its conversion to mechanical power. Due to this fact, we will focus in following our investigation only on the motor type load.

From the EMC point of view the DC motors seem to be better than AC motors. By a DC permanent magnet (PM) disc motor simulation, we will show that failing to recognize of EMC knowledge can lead to the unfavorable EMC parameters of these motors.

3. COMPUTER NUMERICAL SIMULATION OF THE MOTOR MAGNETIC FIELD

The design correctness of the PM DC disc motor could be attested by numerical mathematical methods, to find its magnetic field. Figure Fig. 1.

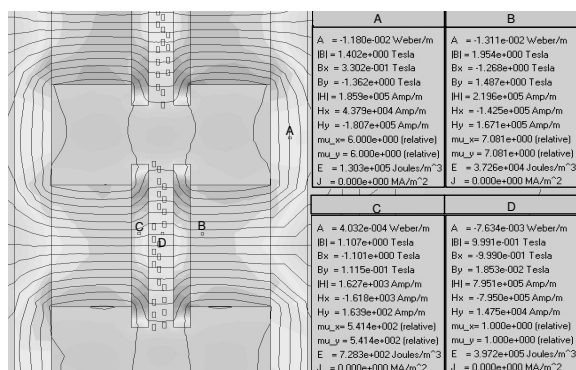


Fig. 1. Motor's magnetic field - simulation

shows the graphical and numerical results of such computer analysis, where a finite element method was used. It is evident, that the motor magnetic field is not closed only inside the motor, but it also reaches its near space and so it must be respected during EMC investigation of the surrounding power electrical engineering systems. The results obtained by such analysis are valid not only for the DC PM disc motors, but also for the rest DC and AC electrical machines.

4. SIMULATION AND MEASUREMENT OF THE MOTOR'S EMC

Let us try to state the motor's EMC. Point A represents the place, where the leakage field between the left and right motor poles is closed. The field is almost homogenous in this place. The position of point B is chosen so, that it is located on one edge of the permanent magnet motor poles. The magnetic field of the motor is periodically located around the motor perimeter. The number of periods corresponds to the number of motor pole pairs. We will also try to find the time change of the magnetic field besides its absolute value, which is caused by the change of its working conditions. This change induces negligible voltages in electrical loops of the surrounding electric circuits. Interesting fact is that the change of magnetic field is created besides the regulation moments also in steady state working condition, if semiconductor converter supplies the motor. Such case is very frequent in modern electrical driving systems. In following we will suppose that the DC PM motor is fed by one quadrant DC voltage impulse converter. The equivalent electrical scheme of the DC motor can be represented by serial connection of a resistor, inductor and an induced voltage source. The shape of the feeding current will be non-constant. The measured curves of switching transistor voltage u_{CE} and the load current i_Z are shown in figure Fig. 2. Figure Fig. 3, displays the curves of the transistor (IGBT) voltage u_{CE} and current i_C .

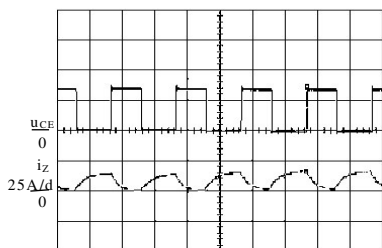


Fig. 2. The measured voltage u_{CE} and motor current i_Z

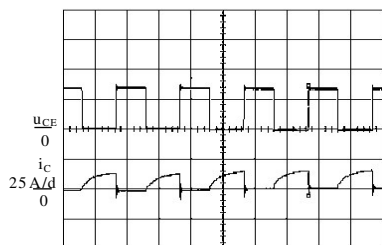


Fig. 3. The measured voltage u_{CE} and motor current i_C

The sampled data of the load current i_Z are listed in table Tab. 1.

Tab. 1. The sampled data of load current i_Z , magnetic field inductions and induced voltages

t [μ s]	i_Z [A]	B_A [T]	B_B [T]	u_{iA} [V]	u_{iB} [V]
0	0	1,485E-01	2,848E-01	0	0
50	5	1,482E-01	2,847E-01	-0,03	-0,01
100	8	1,480E-01	2,846E-01	-0,02	-0,01
150	9,7	1,479E-01	2,846E-01	-0,01	0
200	11,2	1,478E-01	2,846E-01	-0,01	0
250	12,4	1,478E-01	2,845E-01	0	-0,01
300	13,3	1,477E-01	2,845E-01	-0,01	0
350	14	1,477E-01	2,845E-01	0	0
400	14,4	1,477E-01	2,845E-01	0	0
450	14,7	1,476E-01	2,845E-01	-0,01	0
500	15	1,476E-01	2,845E-01	0	0
550	10	1,479E-01	2,846E-01	0,03	0,01
600	7	1,481E-01	2,846E-01	0,02	0
650	5,3	1,482E-01	2,847E-01	0,01	0,01
700	3,8	1,483E-01	2,847E-01	0,01	0
750	2,6	1,484E-01	2,847E-01	0,01	0
800	1,7	1,484E-01	2,847E-01	0	0
850	1	1,485E-01	2,847E-01	0,01	0
900	0,6	1,485E-01	2,848E-01	0	0,01
950	0,3	1,485E-01	2,848E-01	0	0
1000	0	1,485E-01	2,848E-01	0	0

The magnetic field numerical analysis will be done for two extreme values of load current i_Z in the next step. For $I = 0$ A and $I = 15$ A. If the difference of the obtained magnetic field values, corresponding to the above mentioned currents, will be multiplied by the loop area size $S = 0,1 \times 0,05$ m of the other electrical circuit and divided by the time difference, in which the individual current was sampled, then we can obtain imagine about the interference of the induced voltage.

The resulting magnetic field values are shown in figure Fig. 4 for the current i_Z value $I = 0$ A and in places of both investigated points.

The results for the same geometric and material conditions are shown in figure Fig. 5., but at the moment of maximal load current i_Z magnitude. It means at middle of switching period when the

current has the value $I = 15$ A.

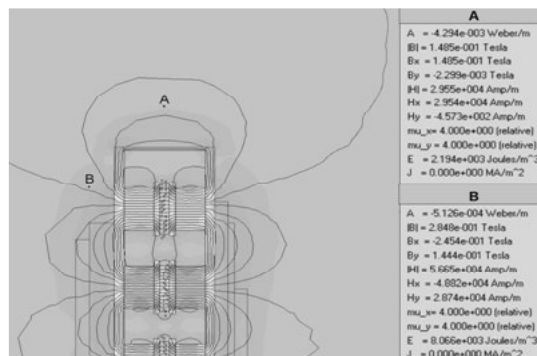


Fig. 4. The motor's magnetic field ($I = 0$ A)

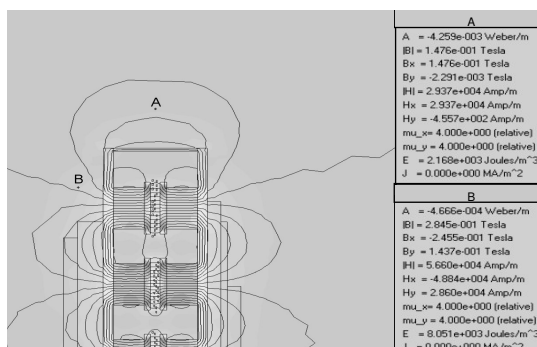


Fig. 5. The motor's magnetic field ($I = 15$ A)

The graphical interpretation of magnetic induction B in time dependence is pictured in figures Fig. 6 and Fig. 7. The induced voltage u_i curves are shown in figures Fig. 8 and Fig. 9.

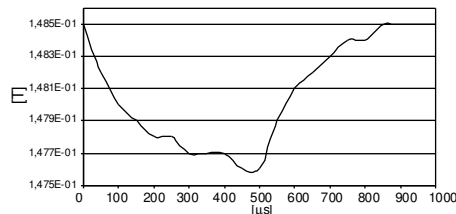


Fig. 6. Magnetic induction B at point A

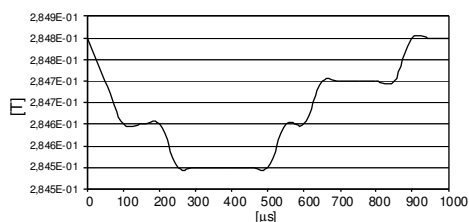


Fig. 7. Magnetic induction B at point B

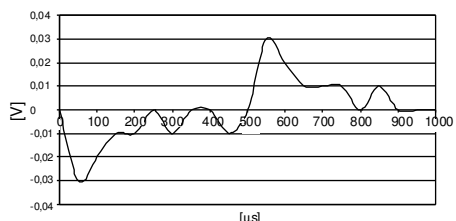


Fig. 8. Induced voltage u_i at point A

Based on the presented facts, it is possible to find out that the biggest magnitude of induced voltage is during the time of the biggest slope of the current motor growth or fall in position A. It appears at the moments of growing and falling edges of feeding

voltage impulse generated by the converter.

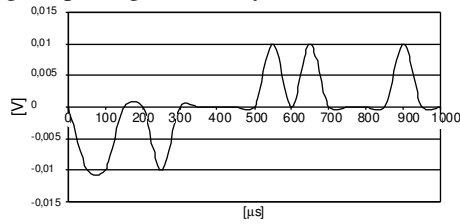


Fig. 9. Induced voltage u_i at point B

The induced voltage peaks reach values up to 30 mV. We must take under consideration, that the induced voltage is generated during the working frequency of 1 kHz. If the converter's working frequency will be higher, the growing and falling time of the current will be smaller, then the induced voltage will be higher. Due to this fact the EMC of the motor will be worse. However, the mentioned dependence of induced voltage on frequency is not linear.

Practical measuring of the magnetic induction B at the chosen place A, where the magnetic field magnitude obtained by simulation is the worst, did verify the correctness of the results obtained by simulation. The measured curve of the magnetic induction B in position A is displayed in figure Fig. 10 together with the curve of transistor current i_c .

The figure Fig. 11. display the curves of induced voltage and current i_c . Induced voltage was sensed by the conductor sensing loop with a rectangle shape and area S ($S = 0,1 \times 0,05$ m).

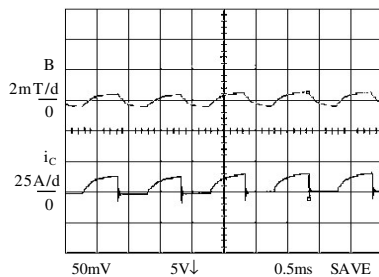


Fig. 10. The measured curves of values B and i_c

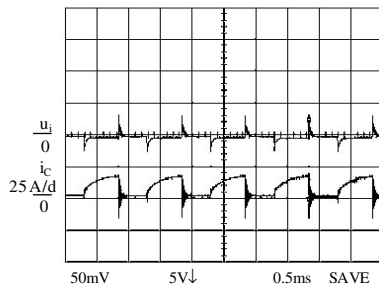


Fig. 11. The measured curves of values u_i and i_c

5. WAYS FOR IMPROVING MOTOR'S EMC

The improvement of EMC of the motors can be done either by a request for reduction of absolute value of leakage magnetic field induction B or by a request for change reduction of variable magnetic inductance in a given place, which is caused by variable working conditions of electrical machine.

The choice of suitable shielding cover is one way

how to improve its EMC. The task of the first cover with relatively great magnetic resistance (with the smallest relative permeability) is to reduce the magnitude of leakage magnetic field. The task of the second shielding cover with relatively small magnetic resistance (with the biggest relative permeability) is on the other hand to create the connection to short for the rest reduced leakage flux.

The designed construction of motor shielding was analyzed by computer simulation. As the first shielding cover material the cooper ($\mu_r = 0,9999935$) with the thickness 2 mm was used. The second cover created by supermaloy ($\mu_r = 529095$) had also the thickness 2 mm. The simulation was done again for current values of $I = 0$ A and $I = 15$ A. The obtained results are shown in figures Fig. 12 and Fig. 13.

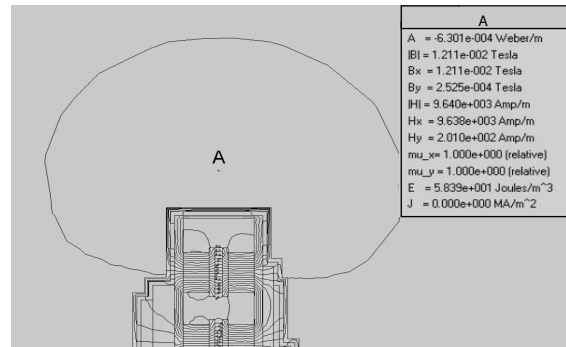


Fig. 12. Shielded DC PM disc motor, $I = 0$ A

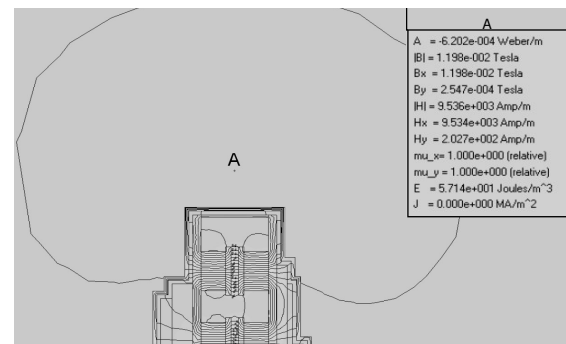


Fig. 13. Shielded DC PM disc motor, $I = 15$ A

By comparing the obtained results with the values in figures Fig. 4 and Fig. 5 we can find out, that the magnetic inductance B value was reduced from value 0,1485 T at new one 0,01211 T under motor current value $I = 0$ A. It means one rank down. The magnetic inductance B value was similarly reduced for the current value $I = 15$ A from 0,1476 T to 0,01198 T. The change of the magnetic inductance, caused by the current change, was reduced from the value of $\Delta B = 0,0009$ T, in the case of the motor without shielding, to $\Delta B = 0,00013$ T, for motor with shielding cover.

The advantage of the proposed solution consists in its simple realization and possibility of shielding cover reduction in dependence on converter's working frequency. If the frequency will be higher, the depth of electromagnetic wave penetration δ will be smaller and so smaller can be also the thickness of the material needed for its damping.

On contrary, the disadvantage of the proposed solution consists in the weight, volume and motor price increasing.

The other way, how to fulfil the requirement of the motor's EMC improvement, is the increasing of the numbers of rotors (under the same motor power) so, that the pole pairs of all (in our case three) rotors, which are placed at a given stator frame yoke position, have mutually opposite oriented poles. The material with a great magnetic resistance (for example copper) mutually separates individual rotor magnetic circuits. To compare the proposed solutions effect, it is necessary to investigate the

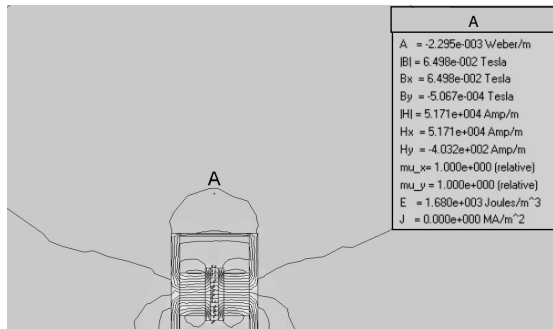


Fig. 14. The motor's magnetic field, $I = 0$ A

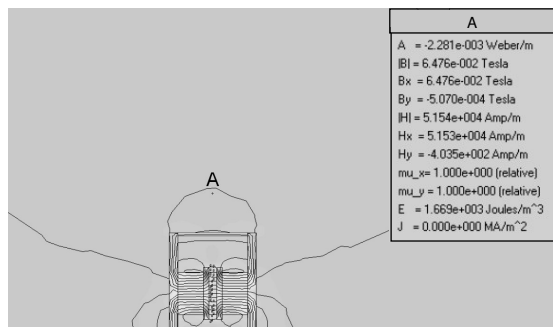


Fig. 15. The motor's magnetic field, $I = 15$ A

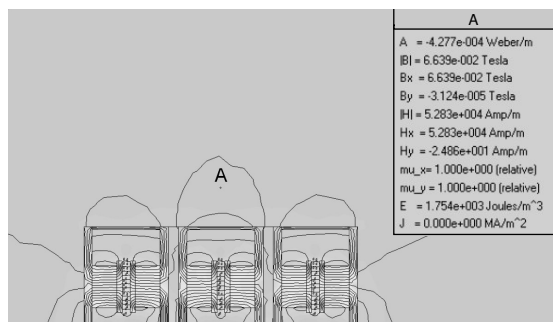


Fig. 16. The three rotors magnetic field, $I = 0$ A

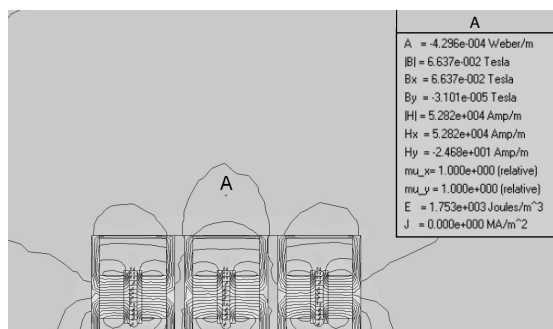


Fig. 17. The three rotors magnetic field, $I = 15$ A

arrangement of the motor magnetic field with simplified stator frame yoke first. The results obtained by the simulation are shown in figures Fig. 14 and Fig. 15.

The results obtained by the simulation for the proposed motor construction with three rotors and improved EMC are displayed in figures Fig. 16 and Fig. 17.

6. CONCLUSION

By comparison of the obtained values with the values in figures Fig. 4. and Fig. 5. we can find out, that the magnitude of magnetic inductance B was reduced from the value of 0,1485 T to a new one 0,006639 T under the current $I = 0$ A. The magnetic inductance B value was similarly reduced for the current value $I = 15$ A from value 0,1476 T to a new one 0,006637 T. The change of the magnetic inductance, caused by motor current change, was reduced from the value of $\Delta B = 0,0009$ T to a new one $\Delta B = 0,000002$ T. The resulting improvement was reached by the fact, that for the same motor power, the motor with higher number of rotors requires smaller motor current and also by the fact, that the leakage magnetic fields of individual poles are mutually subtracted and due to the amount of magnetic field absolute value in the surroundings of the motor has fallen too. Motors constructed in such way are advantageous for utilizing in places, which require improved EMC parameters.

Acknowledgement

The paper has been prepared under support of Slovak grant projects VEGA 1/4174/2007, 1/0660/08, KEGA 3/5227/07, 3/6388/08.

REFERENCES

- [1] Kováčová I., Kaňuch J., Kováč D.: *Electromagnetic compatibility of the power electrical engineering systems*. Equilibria Publishing, Košice, pages 182, 2005.
- [2] Göksu, H., Wunsch, D. C.: *Neural Networks Applied to Electromagnetic Compatibility Simulations*. Lecture Notes in Computer Science, Springer - Verlag GmbH, Vol. 2714, 2003, pp. 1057-1063.
- [3] Mayer D., Ulrych B., Škopek M.: *Electromagnetic Field Analysis by Modern Software Products*. Journal of Electrical Engineering, Vol. 7, No.1, 2001.
- [4] Dobručký B., Ráček V., Špáňik P., Gubric R.: *Výkonové polovodičové štruktúry*. Žilina, 1995.
- [5] Kováčová I., Kováč D., Kaňuch J.: *EMC from the look of theory and application*. BEN – technical literature Publisher, Praha, 164 pages, 2006.
- [6] Michalčík, J., Buday, J.: *Elektrické stroje*. Žilina, 2006.